East European Journal of Physics. 4. 153-163 (2022)
DOI:10.26565/2312-4334-2022-4-15 ISSN 2312-4334

SENSITIVITY AND EVANESCENT FIELD STUDY OF A UNIAXIAL ANISOTROPIC PLANAR WAVEGUIDE BASED OPTICAL SENSOR[†]

Abdelbaki Cherouana[a], Idris Bouchama[b,c], Abdelhalim Bencheikh[d], Samah Boudour[e,*], Muhammad Saeed Akhtar[f]

[a]*Research Unit in Optics and Photonics – University of Sétif 1, Center for development of advanced technologies, Algiers, Algeria*
[b]*Department of Electronic, Faculty of Technology, University of Msila, Msila, Algeria*
[c]*Research Unit on Emerging Materials (RUEM), University Ferhat Abbas, Setif, Algeria*
[d]*Department of Electromechanics, University of BBA, Algeria*
[e]*Research Center in Industrial Technologies CRTI, P.O. Box 64, Cheraga 16014, Algiers, Algeria*
[f]*Department of Physics, University of Education, Lahore, 54770, Pakistan*
**Corresponding authors: Dr. Samah Boudour, Research Center in Industrial Technologies CRTI, P.O. Box 64, Cheraga, 16014, Algiers, Algeria. E-mail: s.boudour@crti.dz*
Received August 24, 2022; revised September 6, 2022; accepted September 11, 2022

The effect of source, geometrical and physical parameters of slab waveguide on the sensitivity of optical sensor and its evanescent field have been investigated. The wave guiding film was the $LiNbO_3$ and the observations revealed that, the maximal sensitivities of Transverse Magnetic (TM) modes and their corresponding frequencies are greater than those for Transverse Electric (TE) modes. Furthermore, the optimal source parameters improve the maximal sensitivity and evanescent field in the cover. However, the increment in the core thickness reduces the sensitivity of sensor due to reduction in evanescent field in the cover. The sensitivity of sensor was observed as a function of refractive indices of cover, core and the substrate. The increase in refractive indices of cover and core, directly affect the sensitivity while an inverse relation has been observed regarding increase in the refractive index of the substrate. It is worth noting that, any changes in the physical parameters of waveguide sensor show insignificant effect on the evanescent fields.
Keywords: Planar waveguide sensor; Birefringence; Source parameters; Geometrical and physical parameters; Sensor sensitivity; Evanescent field
PACS: 42.25.-p, 42.25.Bs, 42.82.Et, 87.85.fk, 07.07.Df, 42.82.-m, 42.81.Gs, 42.79.Pw

Planar waveguide based optical sensors use the exponential decay of evanescent field in the external medium, to sense alterations occurring in the vicinity of a waveguide surface. This feature makes evanescent wave based optical sensor enable monitoring of chemical and biochemical interactions in real-time with high sensitivity and stability. Furthermore, sensors based on optical LOC systems would sense selective analytes just by choosing the appropriate biological receptors [1]. Recently, it has been reported that plasmonic and silicon photonics-based biosensors are among the most employed evanescent-wave biosensors to analyze nucleic acids with potential applicability in the clinical diagnosis [2]. In addition, Lithium Niobate (LN) is among one of the widely used materials for integrated sensor applications due to its excellent optical, ferroelectric, piezoelectric, and thermoelectric properties [3]. In fact, the fabrication of $LiNbO_3$ thin film crystals exhibiting optical properties comparable to those for bulk crystals along with coupled TE and TM modes [4]. Sensitivity, being most important parameter of an optical sensor has attracted significant research interest [5-7]. Thus, planar waveguides comprising left-handed material (LHMs) with different configurations [8], as well as binary and ternary photonic crystal with LHMs layers [9, 10]; have been investigated as optical sensors. It has also been observed that the sensitivity of the proposed structures can be significantly improved by the optimization of physical and geometrical parameters of the waveguide layers.

In this paper, the sensitivity and evanescent fields of a slab waveguide sensor constituted of uniaxial anisotropic crystals have been investigated. The influence of light source in addition to the physical and geometrical parameters of the waveguide, on the sensor sensitivity and evanescent fields have been studied in detail for the two kinds of modes propagating simultaneously in a waveguide. In our previous work [11], the influence of physical parameters was briefly studied.

THEORETICAL MODELING

The planar waveguide for an optical sensor was constituted by three layers of uniaxial crystals of lossless and non-magnetic materials, as presented in Fig. 1. The core refractive index tensor is $\overline{\overline{n_f}}$, whereas, the refractive index tensors of the media above and below the film guide are, respectively, $\overline{\overline{n_c}}$ and $\overline{\overline{n_s}}$. Then:

$$\bar{\bar{n}}_i = \varepsilon_0 \begin{bmatrix} n_i^2 & 0 & 0 \\ 0 & n_i^2 & 0 \\ 0 & 0 & n_{iz}^2 \end{bmatrix},$$

where, i = c, f, s (cover, film, substrate), ε_0 is the dielectric constant of vacuum, $n_i = n_{ix} = n_{iy}$,n_{iz} are, ordinary and extraordinary refractive indices of each layer, respectively.

[†] ***Cite as***: A. Cherouana, I. Bouchama, A. Bencheikh, S. Boudour, and M.S. Akhtar, East Eur. J. Phys. **4**, 153 (2022), https://doi.org/10.26565/2312-4334-2022-4-15

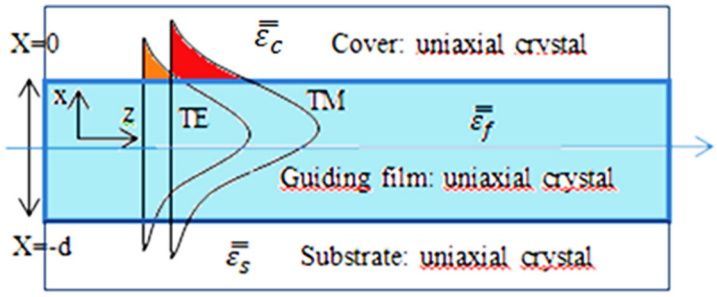

Figure 1. Uniaxial anisotropic slab waveguide-based sensor

Two waves (TE and TM) are propagated separately in the core of such slab waveguide, considered as an ordinary and extraordinary wave, respectively [12].

Sensitivity of a Birefringent Planar Waveguide Based Sensor

The sensitivity is defined as the rate of change in modal effective refractive index relative to the cover refractive index:

$$S = \left(\partial n_p / \partial N\right)^{-1}, \tag{1}$$

The two expressions of the sensor sensitivity for both TE and TM modes are given as [12]:

$$S_{TE} = \sqrt{\frac{1-a_c}{1-X}}\frac{X}{a_c}\frac{1}{\sqrt{a_c-X}}\frac{1}{\left[T+\frac{1}{\sqrt{a_s-X}}+\frac{1}{\sqrt{a_c-X}}\right]}, \tag{2}$$

where

$$T = k_0 d n_f = \frac{arctan\sqrt{\frac{a_s-X}{X}}+arctan\sqrt{\frac{a_c-X}{X}}+m\pi}{\sqrt{X}}. \tag{3}$$

For TE modes

$$S_{TM} = \frac{\frac{X(1-2X+a_c)\sqrt{1-a_c}}{\sqrt{1-X}\sqrt{a_c-X}[a_c(1-X(1-Xa_{cz}))-Xa_{cz}]}}{\left[T'K+\frac{a_c(1-a_c)}{\sqrt{(a_c-X)}[a_c(1-X(1-Xa_{cz}))-Xa_{cz}]}+K\sqrt{\frac{1-a_{sz}}{1-a_s}}\frac{a_s(1-a_s)}{\sqrt{(a_s-X)}[a_s(1-X(1-Xa_{sz}))-Xa_{sz}]}\right]}, \tag{4}$$

where

$$T' = k_0 d n_{fz} = \frac{arctan\frac{1}{\sqrt{1-a_c}\sqrt{1-a_{cz}}}\sqrt{\frac{a_c-X}{X}}+arctan\frac{1}{\sqrt{1-a_s}\sqrt{1-a_{sz}}}\sqrt{\frac{a_s-X}{X}}+m\pi}{\sqrt{X}}. \tag{5}$$

For TM modes,

$$a_s = 1-\frac{n_s^2}{n_f^2};\ a_c = 1-\frac{n_c^2}{n_f^2};\ X = 1-\frac{N^2}{n_f^2};\ a_{sz} = 1-\frac{n_{sz}^2}{n_{fz}^2};\ a_{cz} = 1-\frac{n_c^2}{n_{fz}^2};\ K = \frac{n_{fz}}{n_f},$$

N is the effective refractive index, m is the mode order, d is the core thickness and k_0 is the free-space wavenumber.
The sensitivity can be expressed as a function of evanescent field intensity [13]:

$$S = \Gamma_s\left[\sqrt{\frac{1-a_c}{1-X}}+2P\left(\sqrt{\frac{1-X}{1-a_c}}-\sqrt{\frac{1-a_c}{1-X}}\right)\right], \tag{6}$$

where, $P = 0$ for TE polarization. However, $P = 1$ for TM polarization.
The intensity of evanescent field can be represented by a confinement factor Γ_s, which is the ratio of an electric field intensity in the sensitive region or layer to the entire mode distribution of the guiding mode [14], defined as:

$$\Gamma_s = \frac{\iint_s |E(x,y)|^2 dxdy}{\iint_\infty |E(x,y)|^2 dxdy}. \tag{7}$$

Fields Distribution in Each Region for TE Modes

Guided TE modes exhibit exponentially decreasing behavior in the cover and substrate, and a sinusoidal behavior in the film region. Afterwards, by using boundary conditions, components of the EM field E_y, H_x and H_z in each region as a function of the amplitude can be extracted as [15]:

$$E_y = A\begin{cases} e^{-\gamma_c x} & x \geq 0 \\ \left(cos\gamma_f x - \frac{\gamma_c}{\gamma_f} sin\gamma_f x\right) & -d < x < 0 \\ \left(cos\gamma_f d + \frac{\gamma_c}{\gamma_f} sin\gamma_f d\right) e^{\gamma_s(x+d)} & x \leq -d \end{cases}, \tag{8}$$

$$H_x = \frac{\beta A}{\omega\mu_0}\begin{cases} e^{-\gamma_c x} & x \geq 0 \\ \left(cos\gamma_f x - \frac{\gamma_c}{\gamma_f} sin\gamma_f x\right) & -d < x < 0 \\ \left(cos\gamma_f d + \frac{\gamma_c}{\gamma_f} sin\gamma_f d\right) e^{\gamma_s(x+d)} & x \leq -d \end{cases}, \tag{9}$$

$$H_z = \frac{jA}{\omega\mu_0}\begin{cases} -\gamma_c e^{-\gamma_c x} & x \geq 0 \\ -\gamma_f \left(sin\gamma_f x + \frac{\gamma_c}{\gamma_f} cos\gamma_f x\right) & -d < x < 0 \\ \gamma_s \left(cos\gamma_f d + \frac{\gamma_c}{\gamma_f} sin\gamma_f d\right) e^{\gamma_s(x+d)} & x \leq -d \end{cases}, \tag{10}$$

where

$$\gamma_f = \sqrt{k_0^2 \varepsilon_f - \beta^2}.$$

$$\gamma_c = \sqrt{\beta^2 - k_0^2 \varepsilon_c}.$$

$$\gamma_s = \sqrt{\beta^2 - k_0^2 \varepsilon_s}.$$

Fields Distribution in Each Region for TM Modes

Similarly, different components of the EM field for TM modes can be expressed as:

$$H_y = A\begin{cases} e^{-\gamma_c' x} & x \geq 0 \\ cos\gamma_f' x - \frac{n_f^2}{n_c^2}\frac{\gamma_c'}{\gamma_f'} sin\gamma_f' x & -d < x < 0 \\ \left(cos\gamma_f' d + \frac{n_f^2}{n_c^2}\frac{\gamma_c'}{\gamma_f'} sin\gamma_f' d\right) e^{\gamma_s'(x+d)} & x \leq -d \end{cases}, \tag{11}$$

$$E_x = \frac{\beta A}{\omega\varepsilon_0\varepsilon_i}\begin{cases} e^{-\gamma_c' x} & x \geq 0 \\ cos\gamma_f' x - \frac{n_f^2}{n_c^2}\frac{\gamma_c'}{\gamma_f'} sin\gamma_f' x & -d < x < 0 \\ \left(cos\gamma_f' d + \frac{n_f^2}{n_c^2}\frac{\gamma_c'}{\gamma_f'} sin\gamma_f' d\right) e^{\gamma_s'(x+d)} & x \leq -d \end{cases}, \tag{12}$$

$$E_z = \frac{-jA}{\omega\varepsilon_0\varepsilon_{iz}}\begin{cases} -\gamma_c e^{-\gamma_c' x} & x \geq 0 \\ -\gamma_f' \left(sin\gamma_f' x + \frac{n_f^2}{n_c^2}\frac{\gamma_c'}{\gamma_f'} cos\gamma_f' x\right) & -d < x < 0 \\ \gamma_s' \left(cos\gamma_f' d + \frac{n_f^2}{n_c^2}\frac{\gamma_c'}{\gamma_f'} sin\gamma_f' d\right) e^{\gamma_s'(x+d)} & x \leq -d \end{cases}. \tag{13}$$

The dielectric constant ε_i differs from region to region, *i=c, f, s* (cover, film, substrate).
where

$$\gamma_f' = \sqrt{k_0^2 \varepsilon_{fz} - \beta^2 \frac{\varepsilon_{fz}}{\varepsilon_f}},$$

$$\gamma_c' = \sqrt{\beta^2 \frac{\varepsilon_{cz}}{\varepsilon_c} - k_0^2 \varepsilon_{cz}},$$

$$\gamma_s' = \sqrt{\beta^2 \frac{\varepsilon_{sz}}{\varepsilon_s} - k_0^2 \varepsilon_{sz}}.$$

Influence of Waveguide and Source Parameters on the Sensor Sensitivity and Evanescent Fields

As, the sensitivity expressions and evanescent field components can be expressed as functions of waveguide and the light source parameters. We have developed a program in Matlab tool to observe the influence of physical, geometrical and the source parameters on the sensitivities of TE and TM modes as well as their influence on the evanescent fields in

the cover of a waveguide. For TE mode, H_z and H_x components are observed to be very small as compared to the E_y. However, for TM mode, the dominant components are E_x and E_z, while, H_y is unimportant. For the above said reason, small components are not represented in the figures. Basically, the slab waveguide consists of a core of $LiNbO_3$ on a glass substrate; the wavelength of the source was taken as 650 nm.

Effect of the Source's Parameters

Effect of the Field Amplitude. Equation (6) describes that the sensor becomes more sensitive as the intensity of evanescent field increases, where the intensities of the electric and magnetic evanescent fields are function of their amplitudes.

Fig. 2 illustrates the sensitivity as a function of the frequency for TE_0 and TM_0 modes for different fraction of modal power located in the cover. The observations revealed that, the sensitivity increases with the increase fraction of modal power located in the cover. Though, for TE_0, the sensitivity observed to be maximum for lower frequencies however, decreases for higher frequencies. Whereas, for TM_0, the sensitivity is minimal at lower frequencies while improves at higher frequencies.

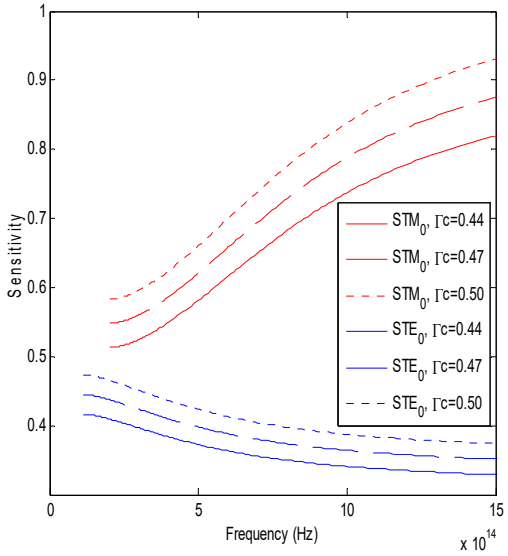

Figure 2. Sensitivity as a function of the frequency for TE_0 and TM_0 modes for different fraction of modal power located in the cover layer, (n_s=1.72, n_c=1.628, d=100 nm, $LiNbO_3$ as guiding film)

The improved sensitivities at higher modal power located in the cover resulted from enhanced amplitudes of evanescent field in the region, as illustrated in Fig. 3 and 4. It has also been observed that, amplitudes of evanescent field components of TM modes are more important than those of TE modes, hence, the sensitivity of TM modes are always greater than that of TE modes.

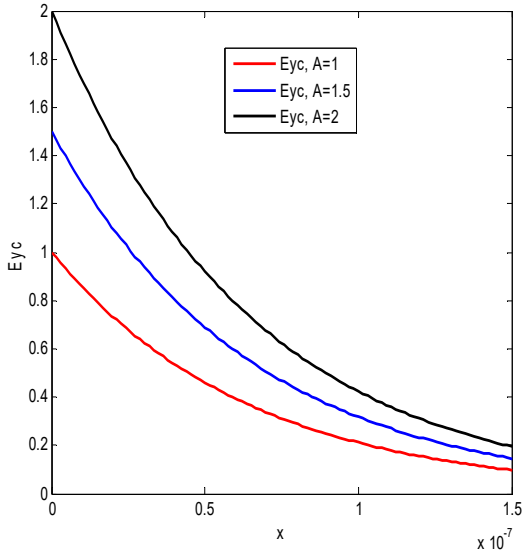

Figure 3. Evanescent field component E_{yc} in the cover versus x of TE_0 mode for different field amplitudes, (n_s=1.72, n_c=1.628, d=100 nm, $LiNbO_3$ as guiding film)

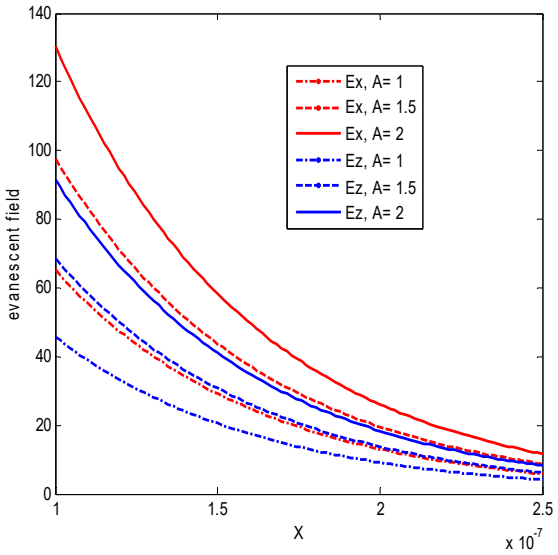

Figure 4. Evanescent field components (E_x, E_z) in the cover versus x of TM_0 mode for different amplitudes of field, (n_s=1.72, n_c=1.628,d=100 nm, $LiNbO_3$ as guiding film)

Effect of the Source's Wavelength. Sensitivities as a function of the core thickness for TE_0 and TM_0 modes, are presented in Fig. 5 observed at different source's wavelengths. The curves show that, sensitivity of the planar waveguide-based sensor increases by increasing the wavelength of source, however, the curves are shifted towards higher core thicknesses. This implies that, at higher wavelengths, maximum sensitivities can be obtained for higher core thicknesses and vice versa.

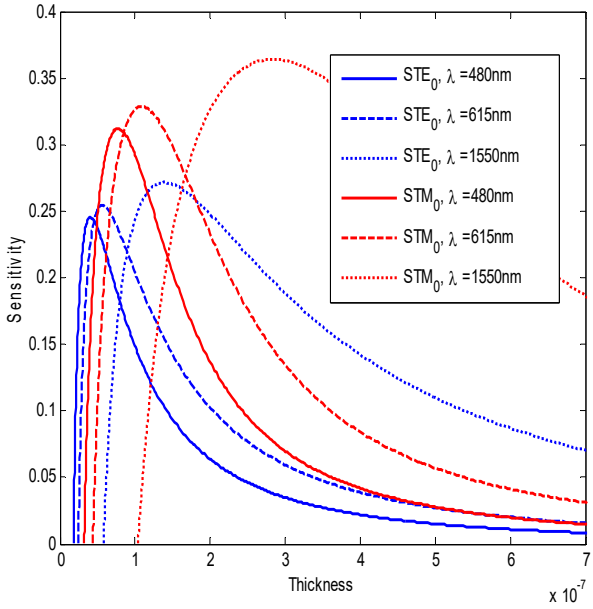

Figure 5 – Sensitivity as a function of the core thickness for TE_0 and TM_0 modes for different wavelength source, (n_s=1.72, n_c=1.628, d=100 nm, $LiNbO_3$ as guiding film)

The increase of the sensitivity for higher source's wavelengths can be justified by an increase in the intensities of evanescent field, as illustrated in Fig. 6 and 7.

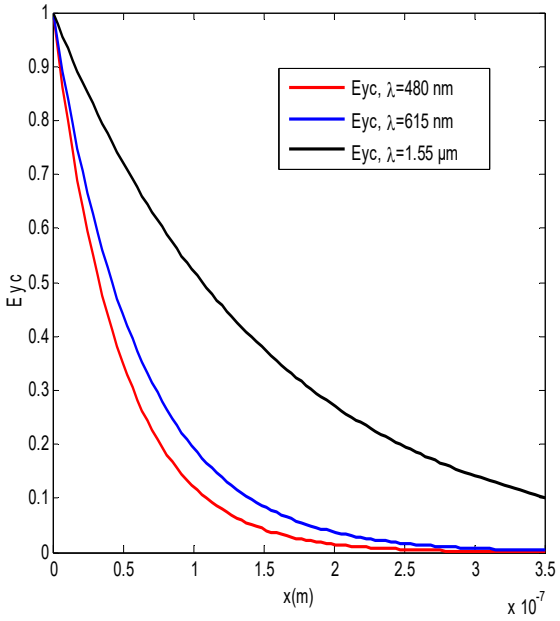

Figure 6. – Evanescent field components E_{yc} in the cover versus x of TE_0 mode for different source's wavelengths, (n_s=1.72, n_c=1.628, d=100 nm, $LiNbO_3$ as guiding film)

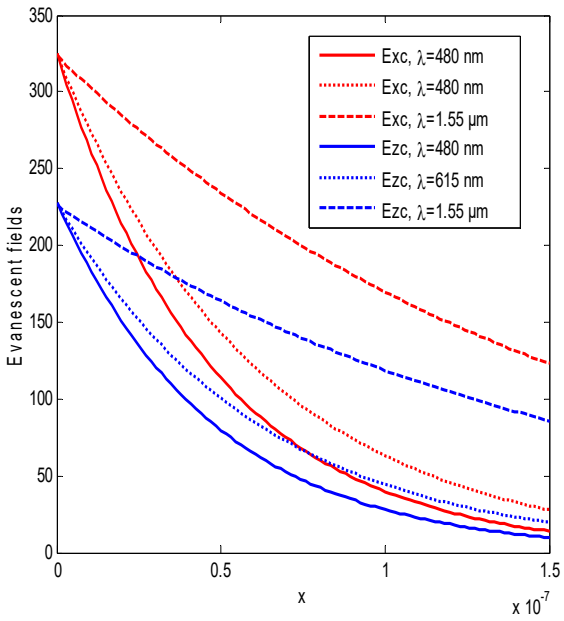

Figure 7. Evanescent field components (E_x, E_z) in the cover versus x of TM_0 mode for different source's wavelengths, (n_s=1.72, n_c=1.628, d=100 nm, $LiNbO_3$ as guiding film)

Effect of the Geometrical Parameter

Fig. 8, represents the sensitivity as a function of the frequency for TE_0 and TM_0 modes at different core thickness. The observations revealed that, by increasing the core thickness, sensitivity of the sensor decreases and curves shifted towards the lower frequencies. The reduced sensitivity is resulted from the decrease in sensing area limited by the evanescent fields, normal to the waveguide at z = 0 and the super surface of the waveguide (x = 0).

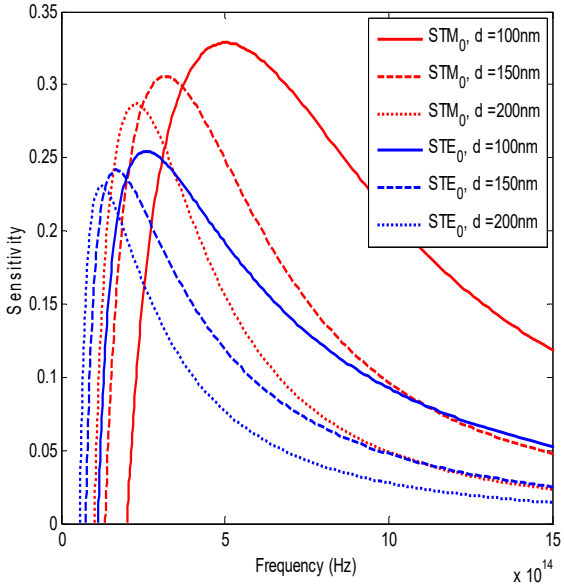

Figure 8. Sensitivity as a function of the frequency for TE_0 and TM_0 modes for different core thicknesses, (n_s=1.72, n_c=1.628, $LiNbO_3$ as guiding film).

In fact, at greater core thickness, maximum part of an optical signal enters into the core of waveguide as energy and ultimately reduces the evanescent field intensities, as illustrated in Fig. 9 and 10.

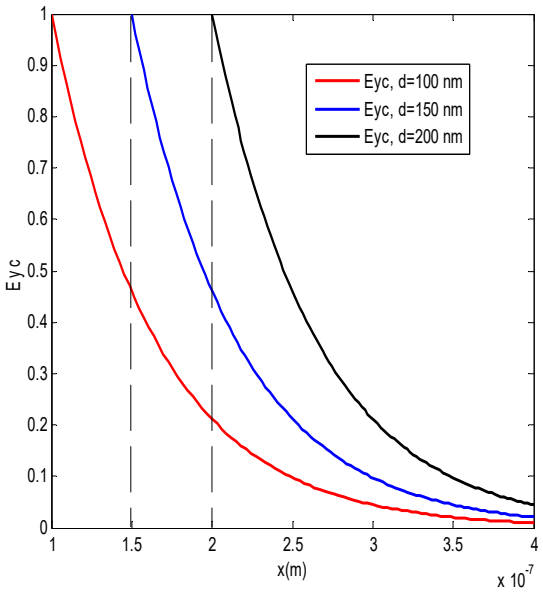

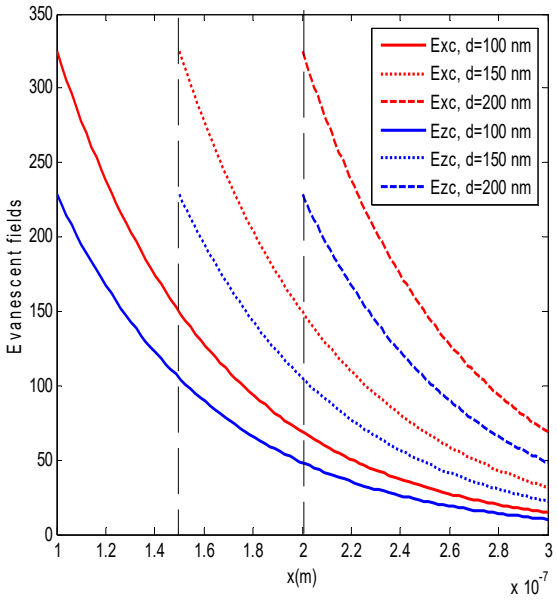

Figure 9. Evanescent field component E_{yc} in the cover versus x of TE_0 mode for different core thicknesses, (n_c=1.628, n_s =1.72, $LiNbO_3$ as guiding film)

Figure 10. Evanescent field components in the cover versus x of TM_0 mode for different core thicknesses, (n_c=1.628, n_s =1.72, $LiNbO_3$ as guiding film)

Effect of the Physical Parameters

Physical parameters studied are the refractive indices of cover, substrate and the core of waveguide. Expressions (2) and (4) demonstrated the influence of physical parameters of waveguide on the sensitivity of the sensor. However, their influence on the evanescent fields are expressed by the electromagnetic field components in the cover.

Effect of the Cover Refractive Index. Fig. 11 illustrated the sensitivities as a function of the frequency of TE_0 and TM_0 modes when the refractive index of cover was taken as 1.48 and 1.70. For TE_0, the observed maximal sensitivities are 0.15 and 0.37, corresponding to the frequencies 3×10^{14} Hz and 1.25×10^{14} Hz, respectively. However, for TM_0, the observed maximal sensitivities are 0.23 and 0.47, corresponding to the frequencies 6.25×10^{14} Hz and 3.25×10^{14} Hz, respectively.

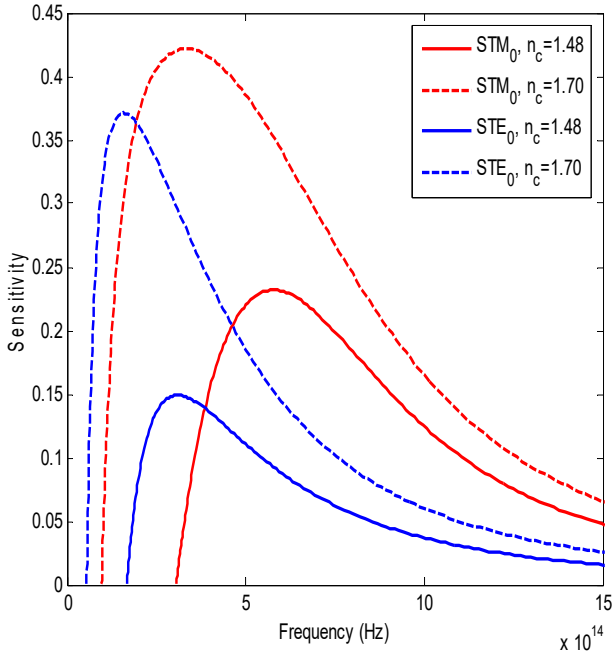

Figure 11. Sensitivity as a function of the frequency for TE_0 and TM_0 modes for different refractive index of the cover material n_c, (n_s=1.72, d=100 nm, $LiNbO_3$ as guiding film)

The curves show that, sensitivity of slab waveguide-based sensor increases by increasing the cover refractive index for both TE and TM modes. In addition to that, the position of maximal sensitivities exhibit shift toward lower frequencies. As the refractive index of cover must be always lesser than that for the substrate, one can conclude that, for both TE and TM modes, the sensitivity of a sensor increases by making the cover refractive index as close as possible to that for the substrate.

Nevertheless, for different cover refractive indices, small changes in the evanescent field components are evident, near to the cut-off frequencies, Fig. 12 and 13. These changes are caused by the variation in effective refractive indices of TE_0 and TM_0 modes induced by fluctuations in core refractive index, Fig. 14. These changes in evanescent field components in the cover, close to cut-off frequencies, have minimal influence on sensitivity of the slab waveguide-based sensor.

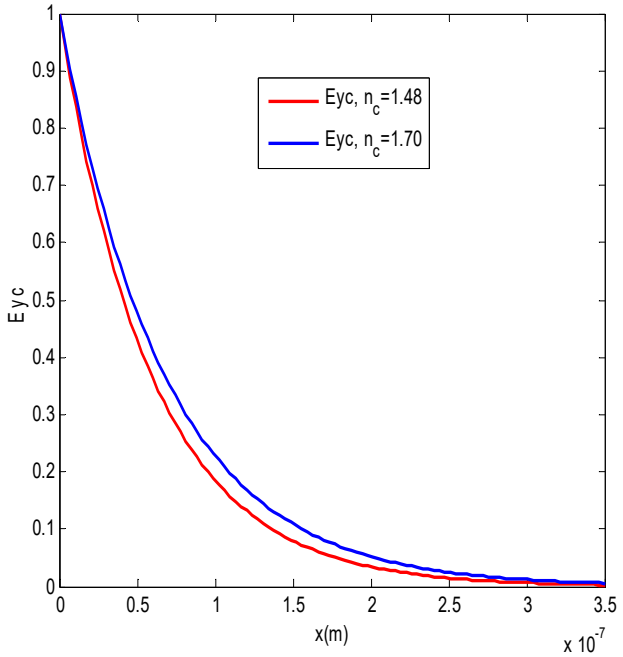

Figure 12. Evanescent field components E_{yc} in the cover versus x of TE_0 mode for different cover refractive indices, (n_s=1.72, d=100 nm, $LiNbO_3$ as guiding film)

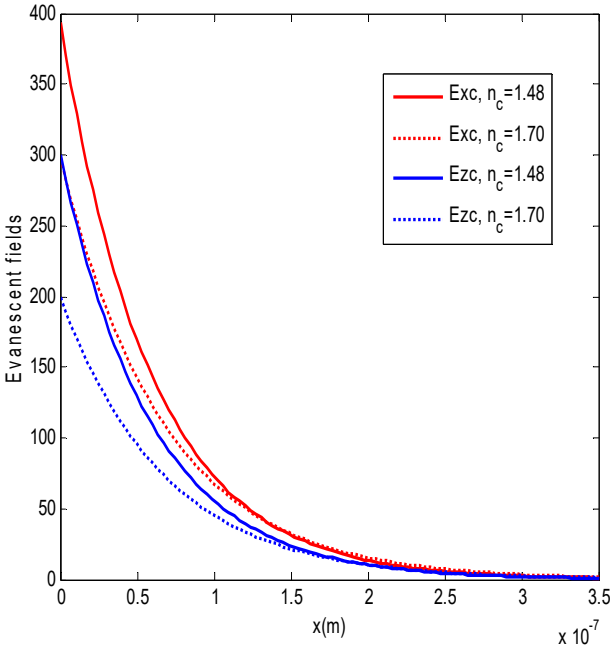

Figure 13. Evanescent field components (E_{xc}, E_{zc}) in the cover versus x of TM_0 mode for different cover refractive indices, (n_c=1.48, d=100 nm, $LiNbO_3$ as guiding film)

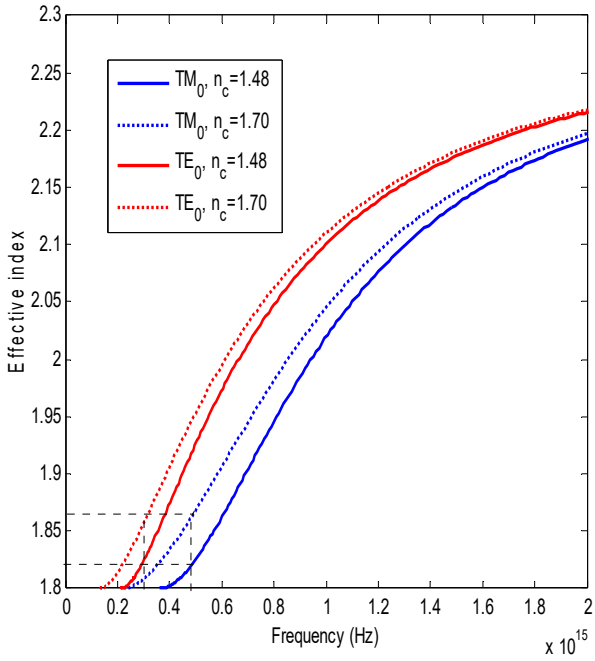

Figure 14. Effective index versus frequency of TE_0 and TM_0 modes in slab waveguide for different cover indices, (n_s=1.72, d=100 nm, $LiNbO_3$ as guiding film)

Effect of the Substrate Refractive Index. Fig. 15 represents the sensitivities of TE_0 and TM_0 modes as a function of the frequency, for various refractive index of substrate. Graphs depicted the maximal values of sensitivities and their corresponding frequencies. For TE_0, maximal sensitivities are observed to be 0.245 and 0.11, corresponding to 2 x 10^{14} Hz and 4 10^{14} Hz frequency, respectively. For TM_0, maximal sensitivities are 0.34 and 0.175, corresponding to the frequencies as 5 10^{14} Hz and 6 10^{14} Hz, respectively. The sensitivity of sensor decreases as a function of substrate refractive index for both TE and TM modes. Furthermore, the position of maximal sensitivities exhibit shifts toward higher frequencies.

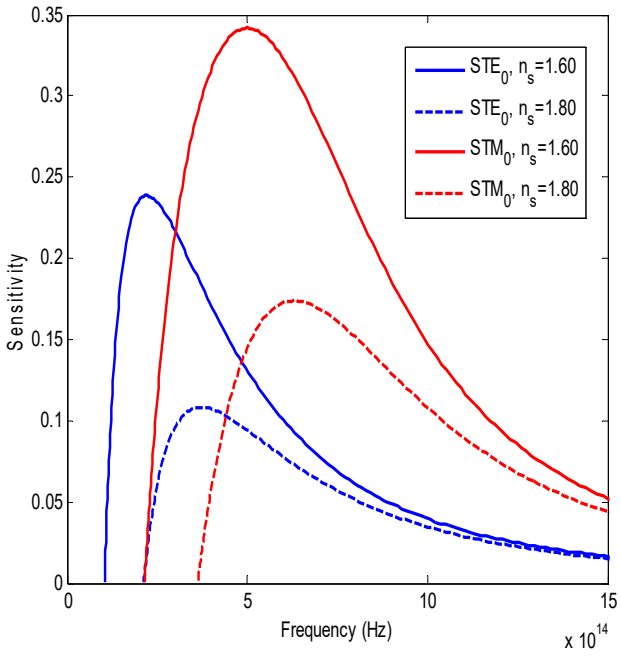

Figure 15. Sensitivity as a function of the effective index for TE_0 and TM_0 modes for different refractive index of the substrate n_s, (n_c=1.48, d=100 nm, $LiNbO_3$ as guiding film)

Evanescent field components of TE_0 and TM_0 modes, for different substrate refractive indices are depicted in Fig. 16 and 17 respectively.

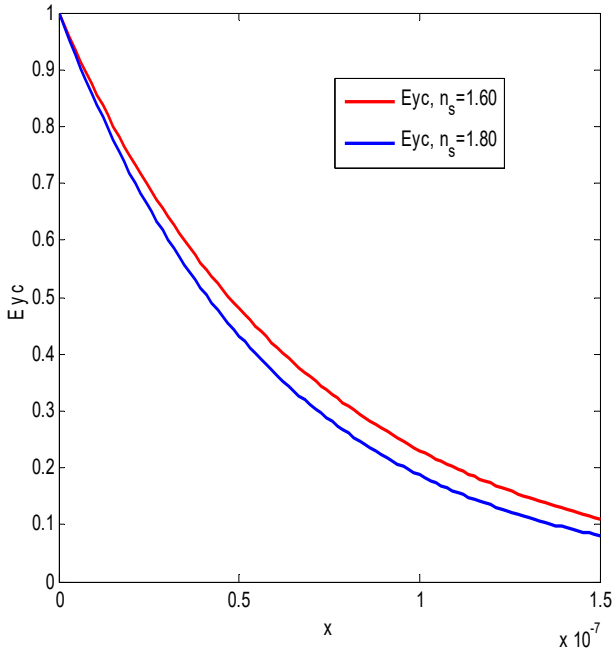

Figure 16. Evanescent field components E_{yc} in the cover versus x of TE_0 mode for different substrate refractive indices, (n_c=1.48, d=100 nm, $LiNbO_3$ as guiding film)

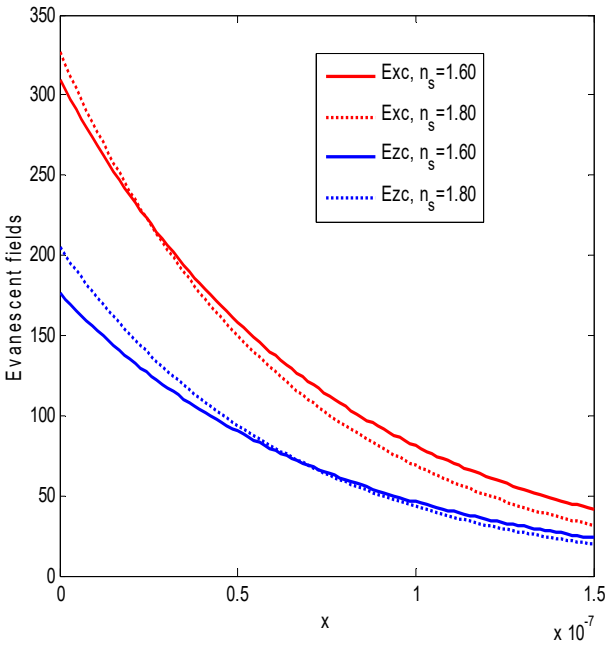

Figure 17. Evanescent field components (E_x, E_z) in the cover versus x of TM_0 mode for different substrate refractive indices, (n_c=1.48, d=100 nm, $LiNbO_3$ as guiding film).

Curves show a small change in the evanescent field components caused by of the variation in refractive index of substrate; and, these small changes occur near the cut-off frequencies of each mode. Far from these frequencies, there has been no changes in evanescent field components. However, these changes are caused by small variation in effective refractive indices of substrate, Fig. 18. One can conclude that, change in evanescent field have negligible influence on the sensitivity of a slab waveguide sensor Fig. 15.

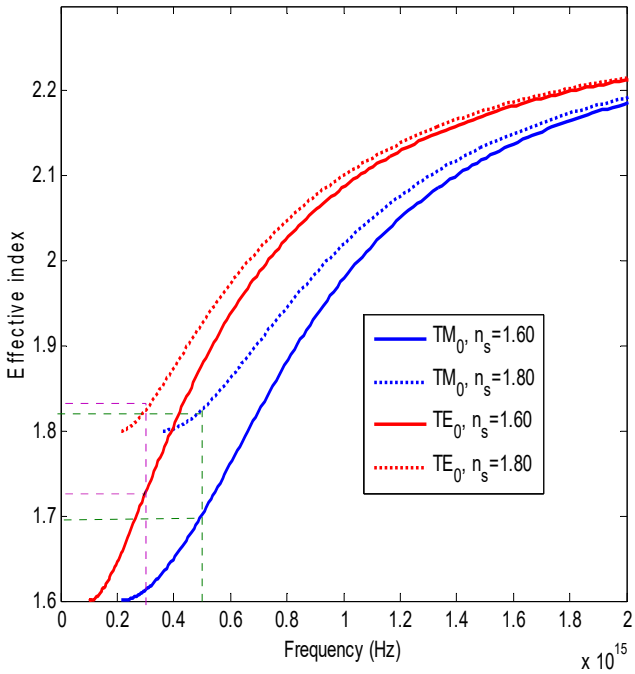

Figure 18. Effective index versus frequency of TE_0 and TM_0 modes in slab waveguide for different substrate refractive indices, (n_c=1.48, d=100 nm, $LiNbO_3$ as guiding film)

Effect of the Core Refractive Index. The sensitivities of TE_0 and TM_0 modes as a function of the frequency, for different core refractive index are illustrated in Fig. 19.

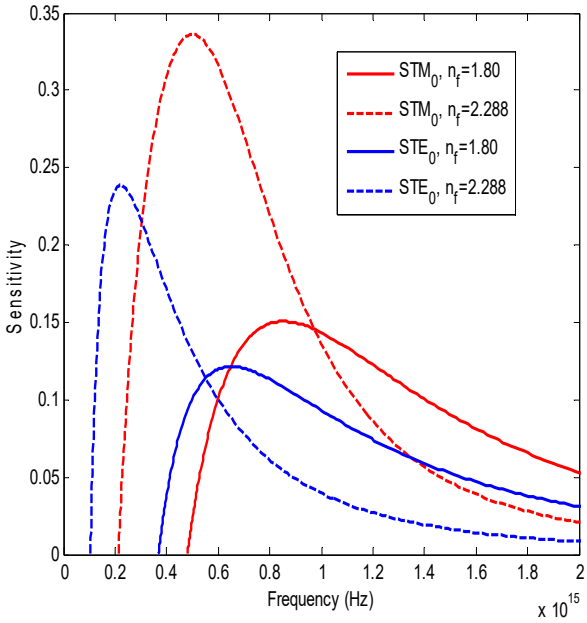

Fig. 19. Sensitivity as a function of the effective index for TE_0 and TM_0 modes for different refractive index of the core n_f, (n_c=1.48, n_s=1.60, d=100 nm,)

For TE_0, maximal sensitivities are observed to be 0.125 and 0.24 corresponding to 6 x 10^{14} Hz and 2 x 10^{14} Hz, respectively. However, for TM_0, maximal sensitivities are 0.15 and 0.34 corresponding to 8 x 10^{14} Hz and 5 x 10^{14} Hz, respectively. The observations revealed that, sensitivity of the planar waveguide-based sensor increases as a function of core refractive index for both TE and TM modes. In addition to that, the position of the maximal sensitivities exhibit shifts toward lower values of frequency.

On the other hand, evanescent field components as illustrated in Fig. 20 and 21 for different core refractive indices, exhibit moderate changes caused by variation in core refractive index; in fact, these changes occur far from the cut-off frequencies of each mode. These changes are caused by the variation in effective refractive indices of TE_0 and TM_0 modes induced at different core refractive index, Fig. 22. These changes in evanescent field, far from the cut-off frequencies, have negligible influence on the sensitivity of a slab waveguide sensor, since the sensitivity peaks appeared near the cut-off frequencies.

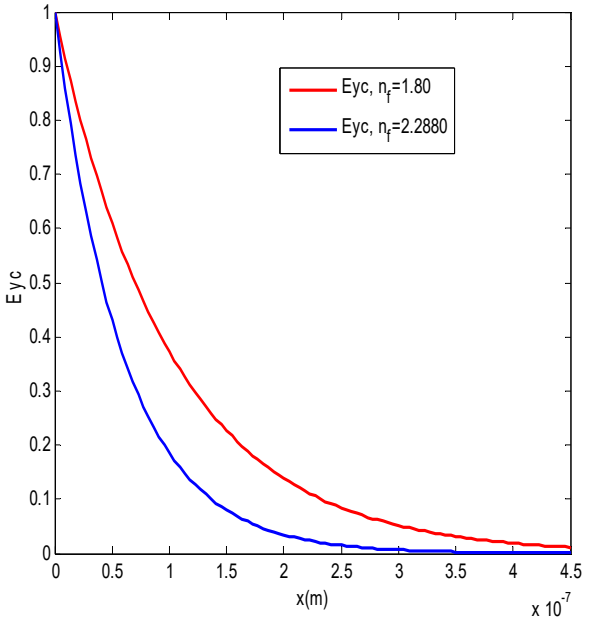

Figure 20. Evanescent field component E_{yc} in the cover versus x of TE_0 mode for different core refractive indices, (n_s=1.60, n_c=1.48, d=100 nm)

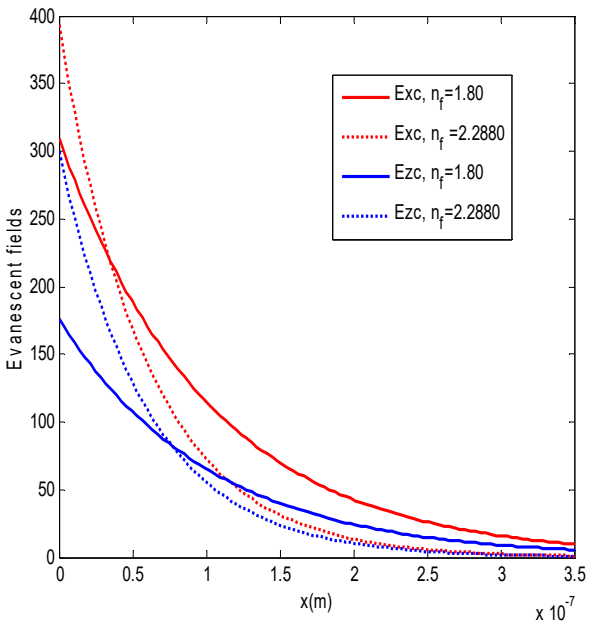

Figure 21. Evanescent field components (E_{xc}, E_{zc}) in the cover versus x of TM_0 mode for different core refractive indices, (n_s=1.60, n_c=1.48, d=100 nm)

CONCLUSIONS

In this work, sensitivity and evanescent field of a planar waveguide-based optical sensor prepared of birefringent materials have been investigated. The influence of source, geometrical and physical parameters of the planar waveguide on the sensitivity of sensor and evanescent field are studied. The observations in all cases revealed that, the maximal sensitivities of TM modes and their corresponding frequencies are greater than those for TE modes. Furthermore, improved sensitivity and evanescent field in the cover has been observed at in higher amplitude and wavelength of the light source. An increase in the core thickness however, reduces the sensitivity of sensor owing to the decrement of evanescent field in the cover. Although, any increment in refractive indices of cover and the core resulted in an improved sensor sensitivity. On the contrary, higher refractive index induces of substrate reduces the sensor sensitivity. The variation in physical parameters of the waveguide sensor have no or negligible influence on the evanescent fields.

ORCID IDs

Abdelhalim Bencheikh, https://orcid.org/0000-0001-7236-4821; **Samah Boudour**, https://orcid.org/0000-0002-4277-6945

REFERECNCES

[1] F.D. Leonardis, and V.M.N. Passaro, "Modeling and Performance of a Guided-Wave Optical Angular-Velocity Sensor Based on Raman Effect in SOI", Journal of Lightwave Technology, **25**(9), 2352 (2007). https://opg.optica.org/jlt/abstract.cfm?URI=jlt-25-9-2352

[2] C.S. Huertas, O. Calvo-Lozano, A. Mitchell, and L.M. Lechuga, "Advanced Evanescent-Wave Optical Biosensors for the Detection of Nucleic Acids: An Analytic Perspective", Front. Chem. **7**, 724 (2019). https://doi.org/10.3389/fchem.2019.00724

[3] T. Kovalevich, D. Belharet, L. Robert, M.S. Kim, H.P. Herzig, T. Grosjean, and M.P. Bernal, "Experimental evidence of Bloch surface waves on photonic crystals with thin-film $LiNbO_3$ as a top layer", Photonics Research, **5**(6), 649 (2017). https://doi.org/10.1364/PRJ.5.000649

[4] P. Rabieia, and P. Gunter, "Optical and electro-optical properties of submicrometer lithium niobate slab waveguides prepared by crystal ion slicing and wafer bonding", Applied Physics Letters, **85**, 4603 (2004). https://doi.org/10.1063/1.1819527

[5] O. Parriaux, and P. Dierauer, "Normalized expressions for the optical sensitivity of evanescent wave sensors: erratum", Optics Letters, **19**(20), 1665 (1994). https://doi.org/10.1364/OL.19.001665

[6] A. Densmore, D.X. Xu, P. Waldron, S. Janz, P. Cheben, J. Lapointe, A. Delâge, B. Lamontagne, J.H. Schmid, and E. Post, "A silicon-on-insulator photonic wire based evanescent field sensor", IEEE Photonics Technology Letters, **18**(23), 2520 (2006). https://doi.org/10.1109/LPT.2006.887374

[7] D. Kumar, and V. Singh, "Theoretical modeling of a nonlinear asymmetric metal-clad planar waveguide-based sensors", Optik **122**(20), 1872 (2011). https://doi.org/10.1016/j.ijleo.2010.12.031

[8] A.A. Alkanoo, and S.A. Taya, "Theoretical investigation of five-layer waveguide structure including two left-handed material layers for refractometric applications", Journal of Magnetism and Magnetic Materials, **449**, 395 (2018). https://doi.org/10.1016/j.jmmm.2017.10.086

[9] S.A. Taya, and S.A. Shaheen, "Binary photonic crystal for refractometric applications (TE case)", Indian Journal of Physics, **92**(4), 519 (2018). https://doi.org/10.1007/s12648-017-1130-z

[10] S.A. Taya, "Ternary photonic crystal with left-handed material layer for refractometric application", Opto-Electronics Review, **26**(3), 236 (2018). https://doi.org/10.1016/j.opelre.2018.05.002

[11] A. Cherouana, A. Bencheikh, and I. Bouchama, "Effect of the electric field induced birefringence on the slab waveguide evanescent-wave sensor sensitivity", Optical and Quantum Electronics, **51**, 331 (2019). https://doi.org/10.1007/s11082-019-2018-2

[12] A.M. Jalaleddine, "Guided waves propagating in isotropic and uniaxial anisotropic slab waveguide", Dissertation, Ohio University U.S.A. 1982.

[13] G.J. Veldhuis, O. Parriaux, H.J.W.M. Hoekstra, and P.V. Lambeck, "Sensitivity enhancement in evanescent optical waveguide sensors", Journal of Lightwave Technology, **18**(5), 677 (2000). https://doi.org/10.1109/50.842082

[14] V.M.N. Passaro, F. Dell'Olio, C. Ciminelli, M.N. Armenise, "Efficient chemical sensing by coupled slot SOI waveguides", Sensors, **9**(02), 1012 (2009). https://doi.org/10.3390/s90201012

[15] G. Lifante, *Integrated Photonics. Fundamentals*, (John Wiley & Sons, England, 2003).

ДОСЛІДЖЕННЯ ЧУТЛИВОСТІ ТА ЕВАНЕСЦЕНТНОГО ПОЛЯ ОПТИЧНОГО СЕНСОРА НА ОСНОВІ ОДНООСНОГО АНІЗОТРОПНОГО ПЛОСКОГО ХВИЛЕВОДУ

Абдельбакі Черуана[a], Ідріс Бушама[b,c], Абдельхалім Бенчейх[d], Сама Будур[e], Мухаммад Саїд Ахтар[f]

[a]*Дослідницький відділ оптики та фотоніки – Університет Сетіфа 1, Центр розвитку передових технологій, Алжир*

[b]*Факультет електроніки, технологічний факультет, Університет Мсіла, Мсіла, Алжир*

[c]*Дослідницький відділ нових матеріалів (RUEM), Університет Ферхата Аббаса, Сетіф, Алжир*

[d]*Факультет електромеханіки, Університет ВВА, Алжир*

[e]*Науково-дослідний центр промислових технологій CRTI, P.O. Бокс 64, Черага 16014, Алжир, Алжир*

[f]*Факультет фізики, Університет освіти, Лахор, 54770, Пакистан*

Досліджено вплив геометричних і фізичних параметрів пластинчастого хвилеводу на чутливість оптичного датчика та його гасне поле. Хвилепровідною плівкою був $LiNbO_3$, і спостереження показали, що максимальна чутливість поперечних магнітних (TM) мод та їхні відповідні частоти вищі, ніж для поперечних електричних (TE) мод. Крім того, оптимальні параметри джерела покращують максимальну чутливість і миттєве поле в обкладинці. Однак збільшення товщини серцевини знижує чутливість сенсора через зменшення спадаючого поля в покритті. Чутливість датчика спостерігали як функцію показників заломлення покриття, серцевини та підкладки. Збільшення показників заломлення покриття та серцевини безпосередньо впливає на чутливість, у той час як спостерігається зворотна залежність щодо збільшення показника заломлення підкладки. Варто зазначити, що будь-які зміни у фізичних параметрах хвилевідного датчика незначно впливають на гаснучі поля.

Ключові слова: планарний хвилевідний датчик; подвійне променезаломлення; параметри джерела; геометричні та фізичні параметри; чутливість сенсора; спадаюче поле